

# Fatigue-Crack Propagation Behavior of Type 304 Stainless Steel at Elevated Temperatures

LEE A. JAMES AND EARL B. SCHWENK, JR.

The fatigue-crack propagation behavior of Type 304 stainless steel was investigated within the framework of linear elastic fracture mechanics at temperatures of 75°, 600°, 1000°, and 1200°F. The cyclic frequency for the elevated temperature tests was 4 cpm. It was found that, in general, fracture mechanics concepts may be used to describe the crack propagation behavior at these temperatures, and that increasing the temperature had a significant effect in increasing the fatigue-crack growth rate.

AUSTENITIC stainless steels are among the prime candidates for structural applications in the liquid-metal fast-breeder type nuclear reactors (LMFBR). The LMFBR's are considered to be representative of one of the types of the next generation of power generating reactors, and it is anticipated that greater overall efficiencies will be realized through the use of these reactors. One of the main reasons for the increased efficiency will be the use of considerably higher operating temperatures than are prevalent in today's generation of pressurized water and boiling water reactors. Sodium or other liquid metals, rather than pressurized water, will be used for the cooling media, and operating temperatures of many of the components are expected to be in the 1000° to 1200°F range. Therefore, knowledge of the fatigue-crack propagation behavior of the austenitic stainless steels in this temperature range will be of value in the design and development of structural components for the LMFBR's.

This paper describes work that has been done in determining the fatigue-crack growth characteristics of AISI Type 304 stainless steel subjected to typical LMFBR operating temperatures. The work has been done in support of the Fast Flux Test Facility program.

## EXPERIMENTAL PROCEDURE

The material used in this investigation was obtained from a special supply of well-characterized materials that the U.S. Atomic Energy Commission maintains to insure that interlaboratory studies will be dealing with the same material. All specimens used in this study were taken from  $\frac{1}{2}$  in. thick plates of AISI Type 304 stainless steel (Allegheny Ludlum Heat No. 55697). The certified chemical analysis and static room temperature mechanical properties for Heat no. 55697 are given in Tables I and II, respectively. The material was in the annealed condition, and the mechanical and thermal history is detailed in the Appendix.

With the exception of specimen no. 3, all of the specimens used in this study were of the single-edge-notch (SEN) configuration. Specimen no. 3 was of the wedge-opening-load (WOL) type, and had the planform dimensions of a standard 1-in. WOL specimen, but was only  $\frac{1}{2}$  in. thick, see Fig. 1 for specimen dimensions. A

jewelers' saw was used to produce a crack-starter notch approximately  $\frac{1}{8}$  in. long in the SEN specimens and the fatigue crack was allowed to initiate from the notch and grow approximately 0.05 in. before crack length measurements were commenced.

All specimens were cycled in uniaxial tension at stress ratios between zero and 0.05, see Table III for test parameters. Two types of fatigue testing machines were employed: an electrohydraulic servocontrolled MTS fatigue machine, and a Baldwin-Tate-Emery universal testing machine (BTE) equipped with a load-cycling attachment. Two cyclic load waveforms were utilized with the MTS machine, (a sawtooth ramp for specimens nos. 1, 4, 5, and a sinusoidal waveform for specimen no. 3), while the BTE machine produced a waveform that approximated a sawtooth ramp, see Fig. 2. Cyclic frequencies were kept low (4 cpm) for the elevated temperature tests since many of the reactor structural loadings of interest do not occur at the higher frequencies. It was found that even at 4 cpm, the loads indicated by the loading dial on the BTE control console were unreliable due to the inertia of the loading system and the response characteristics of the bourdon tube and associated mechanical linkages that comprise the load indicator system. Therefore, a load cell was inserted in the loading train, in series with the specimen and the output of the load cell was used in setting up the cyclic load limits.

Crack lengths were read at approximately 65X with a Gaertner travelling microscope (least dial division 0.0001 in.), and crack length vs cycles data were taken throughout each test. In the case of the elevated temperature specimens, crack length readings were always taken after the specimens had completely cooled to room temperature. Crack length readings were made on each side of the specimen and then averaged. The crack lengths were not corrected for plasticity effects. In general, the increment of crack extension between readings was limited to 1 pct (or less) of the total specimen width. The crack growth rate was calculated for each increment of crack extension, and the stress intensity factor range was based on the average crack length for that increment using

SEN Specimen:

$$K = \sigma \sqrt{\pi a} \left[ 1.12 - 0.23 \left( \frac{a}{w} \right) + 10.55 \left( \frac{a}{w} \right)^2 - 21.71 \left( \frac{a}{w} \right)^3 + 30.38 \left( \frac{a}{w} \right)^4 \right] \quad [1]$$

LEE A. JAMES is Senior Research Engineer, WADCO Corp., Richland, Wash. EARL B. SCHWENK, JR. is Research Engineer, Battelle-Northwest, Richland, Wash.

Manuscript submitted August 10, 1970

Table I. Certified Chemical Analysis of AISI 304 Stainless Steel Allegheny Ludlum Heat No. 55697

	C	Mn	P	S	Si	Cr	Ni	Cu	Mo	Pb	Ca	Sn	Ti	N
Ladle	0.051	0.83	0.020	0.012	0.47	18.30	9.50	0.13	0.09	<0.001	0.11	0.01	<0.01	0.032
Check	0.050	0.88	0.019	0.010	0.50	18.21	9.57	0.21	0.18	<0.001	0.11	0.004	<0.01	0.034
Check	0.050	0.88	0.018	0.010	0.49	18.29	9.53	0.21	0.18	<0.001	0.11	0.006	<0.01	0.024
Check	0.060	0.86	0.019	0.010	0.49	18.26	9.43	0.21	0.18	<0.001	0.11	0.008	<0.01	0.032

Total rare earths <0.001

Table II. Certified Mechanical Properties for AISI 304 Stainless Steel Plate Allegheny Ludlum Heat NO. 55697

0.2 Pct Yield Strength, psi	Tensile Strength, psi	Pct Elongation	Hardness, Bnh	Pct R.A.	G.S. ASTM
39,700	77,100	65	126	60.8	4.5
39,500	77,000	65	126	60.5	4.5

Tensile test conducted per ASTM E8-61T.  
Oxalic acid test satisfactory.  
Bend test satisfactory.

WOL Specimen:

$$K = \frac{P}{t\sqrt{W}} \left[ 29.6 \left( \frac{a}{w} \right)^{0.5} + 655.7 \left( \frac{a}{w} \right)^{2.5} - 1017.0 \left( \frac{a}{w} \right)^{3.5} + 638.9 \left( \frac{a}{w} \right)^{4.5} \right] \quad [2]$$

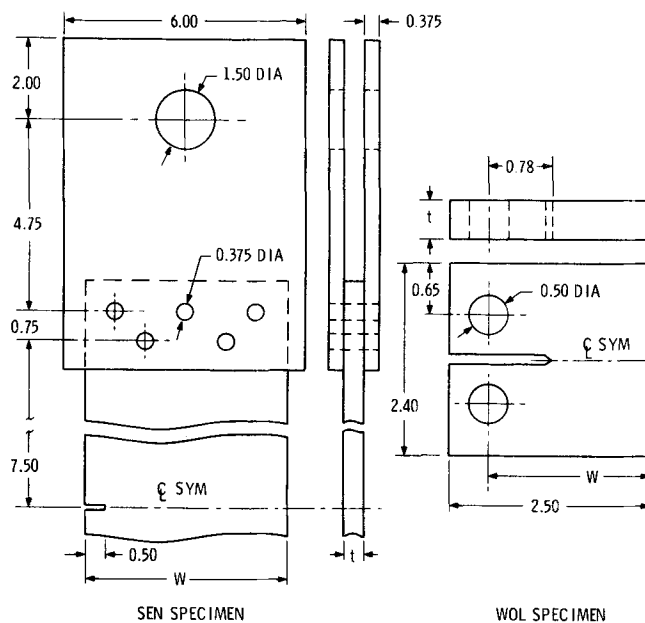
where  $\sigma$  is the uniform gross section stress remote from, and normal to, the crack plane;  $P$  is the tensile load applied to the specimen;  $a$  is the crack length;  $W$  is the specimen width; and  $t$  is the specimen thickness.

Specimens 6 through 10 were tested in air at elevated temperatures corresponding to the anticipated LMFBR operating regime. The specimens were radiantly heated by banks of Research Inc. "Pyropanel" heating fixtures employing quartz lamps. Temperature control was accomplished through the use of Research Inc. "Thermac" control units. Each side of the specimen had three independent zones of temperature control. In addition to the control thermocouples, twelve chromel-alumel thermocouples were placed at various locations on each specimen to monitor the temperature. With this arrangement, it was possible to control the temperature in the vicinity of the crack to within  $\pm 5^\circ\text{F}$ , and temperatures were maintained within approximately  $\pm 20^\circ\text{F}$  over the entire specimen.

The remainder of the tests were conducted under ambient laboratory conditions, and provide the "baseline" data with which to compare the elevated temperature test results. The relative humidity at room temperature ranged between 15 and 45 pct during these tests.

Maximum cyclic load levels were chosen such that the stresses in the net section were well below the yield strength at the end of the test. In general, a test was terminated when either 1) the crack length (SEN specimens) equaled half the specimen width or 2) when the average stress in the net section reached 80 pct of the yield strength at the appropriate test temperature.

Yield strengths were not determined for the elevated temperature cases. However, examination of the multitude of elevated temperature tensile tests listed in Ref. 1 indicated that the lowest reported yield strengths



SPECIMEN NUMBER	SPECIMEN TYPE	t	W	CRACK ORIENTATION
1	SEN	0.491 IN.	4.950 IN.	RW
2	SEN	0.491	4.910	RW
3	WOL	0.494	2.001	RW
4	SEN	0.493	4.915	WR
5	SEN	0.496	4.910	WR
6	SEN	0.494	4.918	WR
7	SEN	0.496	4.898	RW
8	SEN	0.496	4.918	WR
9	SEN	0.497	4.910	RW
10	SEN	0.494	4.921	WR

Fig. 1—Fatigue test specimens. All dimensions in inches.

for Type 304 stainless steel at 1000° and 1200°F were 40 and 39 pct, respectively, of the room temperature values. Using  $\sigma_{ys} = 39,500$  psi (lowest of Table II values), a conservative estimate of 1000° and 1200°F monotonic yield strengths would be 15,800 and 15,400 psi, respectively. With this in mind, maximum gross-section stresses were kept quite low for specimens 6 through 10. Cyclic work-hardening might have raised the yield strength somewhat,<sup>2</sup> but the monotonic yield strengths were used for determining when to terminate a test.

## RESULTS AND DISCUSSION

Although the austenitic stainless steels are widely used in structural applications, little fatigue-crack growth rate data has been published concerning their behavior at either room or elevated temperatures. Brothers<sup>3</sup> has studied the fatigue-crack growth rate be-

Table III. Summary of Test Parameters

Specimen No.	Temp.	Maximum Stress	Stress Ratio	Frequency	Test Machine
1	75°F	9,250 psi	0.004	400 cpm	MTS
2	75	18,980	0	2	BTE
3	75	*	0.050	60	MTS
4	75	9,300	0.004	400	MTS
5	75	18,480	0.002	180	MTS
6	600	8,230	0	4	BTE
7	1000	8,230	0.050	4	BTE
8	1000	5,740	0	4	BTE
9	1200	5,940	0	4	BTE
10	1200	8,230	0	4	BTE

\*Maximum load = 1700 lb.

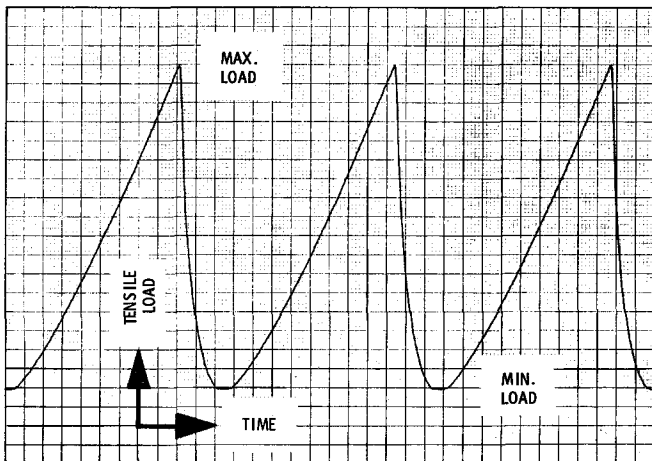


Fig. 2—Typical cyclic waveform for Baldwin-Tate-Emery test machine.

behavior of Type 304 at room temperature, 550° and 650°F, and Hudson<sup>4</sup> has published crack length vs cycles data for Type 301 at room temperature and 550°F (Hudson attempted no correlation between  $da/dN$  and  $\Delta K$ ). Because both Brothers and Hudson used maximum gross-section stress levels at or above  $\sigma_{ys}$ , their data is of doubtful value from the standpoint of linear elastic fracture mechanics.

The test results of this study for 75°, 600°, 1000°, and 1200°F are given in Figs. 3 through 6 as plots of  $da/dN$  vs  $\Delta K$ . The scale of the abscissa is expanded, relative to that of the ordinate, so that any trends (as well as experimental scatter) become more pronounced.

Examination of Fig. 3 reveals that, as might be expected for a cubic material in the annealed condition, there is no noticeable difference in behavior between RW and WR orientations. There is also no apparent effect on fatigue-crack growth rate at room temperature due to differences in either cyclic frequency or waveform. An approximately linear relationship is observed between  $\log(da/dN)$  and  $\log(\Delta K)$ , and the behavior may generally be described by the relationship suggested by Paris and Erdogan<sup>5</sup>

$$da/dN = C(\Delta K)^n \quad [3]$$

where  $da/dN$  = fatigue-crack growth rate;  $\Delta K$  = stress intensity factor range; and  $C$  and  $n$  = constants for a given material-environment combination. A least-squares regression was used to obtain the best fit

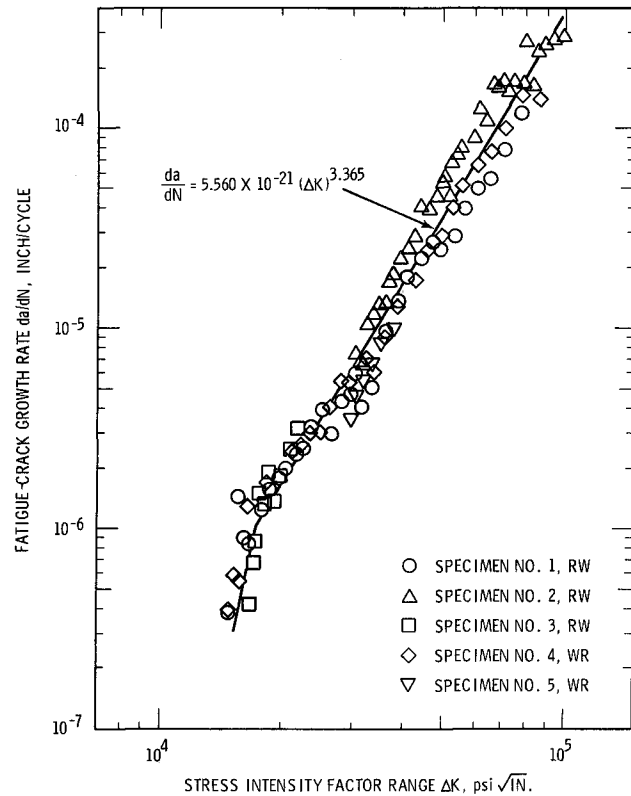


Fig. 3—Fatigue-crack propagation behavior of Type 304 stainless steel at 75°F.

through the data, and this is also shown. It will be noted, however, that the data of three specimens (nos. 1, 3, and 4) indicates that there appears to be a slope transition at a  $\Delta K$  of approximately 17,000  $\text{psi}\sqrt{\text{in}}$ . Since the specimens were precracked at (or below) the test load for approximately 0.05 in. before readings were commenced, it is doubtful that this behavior could be attributed to crack initiation or notch effects. The apparent change in cracking behavior merits further study.

Similar slope transitions have been noted by Paris *et al.*<sup>6</sup> for SAE 9130 steel, by Wilhem<sup>7</sup> for 2024-T3 and 7075-T6 aluminum alloys, by Gurney<sup>8</sup> for mild steel, and by Feeney *et al.*<sup>9</sup> for 2024-T3 and 7075-T6 aluminum alloys. Wilhem<sup>7</sup> attributed the slope transition to a change from a tensile mode to a shear mode, while Gurney<sup>8</sup> suggested that the slope transition was a function of the mean stress. Feeney *et al.*<sup>9</sup> have investigated the slope transition in more detail and have concluded that the transition is not environmentally controlled and reflects some intrinsic feature of the material (possibly involving the plastic zone size, interparticle spacing and material ductility). The present authors concur with Feeney *et al.*<sup>9</sup> regarding the lack of a systematic environmental (*i.e.* temperature) pattern to the transition points. It is difficult, however, to see how plastic zone size could play an important role in explaining the slope transitions observed in this study. At the two temperatures where the transition is most pronounced, 75° and 1200°F, the transition takes place at approximately the same value of  $\Delta K$ . The material yield strengths (and hence plastic zone sizes) are obviously quite different at the two temperatures. The fracture faces for all specimens tested were flat (*i.e.*

normal to the applied stress) and devoid of shear lips. Therefore, the transitions cannot be attributed to a change from a tensile mode to a shear mode.

Figs. 4, 5, and 6 illustrate the behavior at 600°, 1000°, and 1200°F. In general, the "power law" relationship is maintained. Again there is suggestion of a slope transition in all three sets of data. In the case of the data at 600° and 1000°F, the slope transitions have been indicated with question marks since few data points exist at the lower growth rates. However, the authors feel that the lower data points represent valid test values.

It will be seen that in general, the fatigue-crack growth rate increases with increasing temperature. This is generally in accord with the observations of several other investigators for a variety of different materials.<sup>10-13</sup> Between  $\Delta K = 9500 \text{ psi}\sqrt{\text{in.}}$  and  $\Delta K = 12,000 \text{ psi}\sqrt{\text{in.}}$ , the data seems to imply that the crack growth rate is higher at 1000° than at 1200°F. Superposition of the individual data points for both curves shows, however, that the differences are not great and are almost within the scatter of the data.

The contribution of the air environment to the increased crack growth rates at elevated temperatures is unknown, but the crack growth rates are probably higher than those at the corresponding temperature *in vacuo*. The results of Smith *et al.*<sup>14</sup> indicate that at temperatures of 500° and 800°C, the fatigue-crack growth rates of Type 316 stainless steel are approximately an order of magnitude higher at 810 torr oxygen than at  $10^{-6}$  torr oxygen. (Tests were conducted in reversed bending at constant amplitude and crack growth rates were plotted against crack length).

Wei<sup>11</sup> has suggested that it may be possible to repre-

sent the fatigue-crack growth behavior with an Arrhenius-type rate process term,

$$\frac{da}{dN} = A f(\Delta K) \exp \frac{-u(\Delta K)}{kT} \quad [4]$$

where  $A$  = a constant;  $f(\Delta K)$  = crack driving force;  $u(\Delta K)$  = apparent activation energy;  $k$  = Boltzmann's constant; and  $T$  = absolute temperature. Yokobori<sup>15</sup> has also suggested a rate process approach to fatigue-crack propagation, and Ryder and Gallagher<sup>11</sup> have had success in applying a rate process analysis to the fatigue-crack propagation of SAE 4340 steel in distilled water.

The data obtained in this study is presented in the form of an Arrhenius diagram in Fig. 7. Each data point shown represents the value of the least-squares regression at the particular value of  $\Delta K$  under consideration. As may be seen, the data does not fit well with a linear relationship between  $\log (da/dN)$  and  $1/T$ . Fatigue-crack growth rate is obviously a thermally-activated process, although the results of this study indicate that over the wide range of temperatures considered (534° to 1659°R), a single Arrhenius-type rate process term does not adequately represent the behavior. In order for a single rate process term to describe a given phenomenon over some temperature range, a single process must be dominant over that range. Therefore, the present data implies that more than one process is dominant in the fatigue cracking of Type 304 stainless steel over the temperature range 75° to 1200°F.

#### CONCLUDING REMARKS

The results of this study are summarized in Fig. 8. It may be seen that temperature has a profound effect

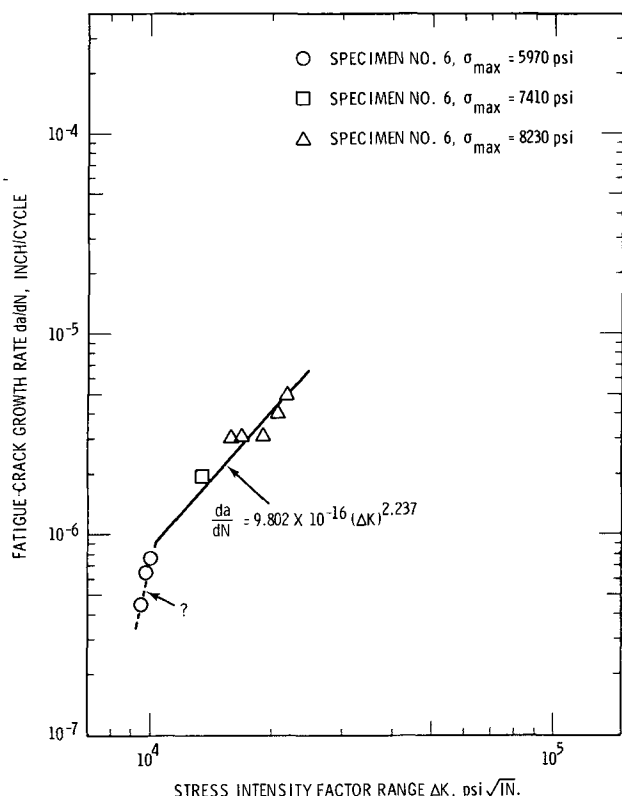


Fig. 4—Fatigue-crack propagation behavior of Type 304 stainless steel at 600°F.

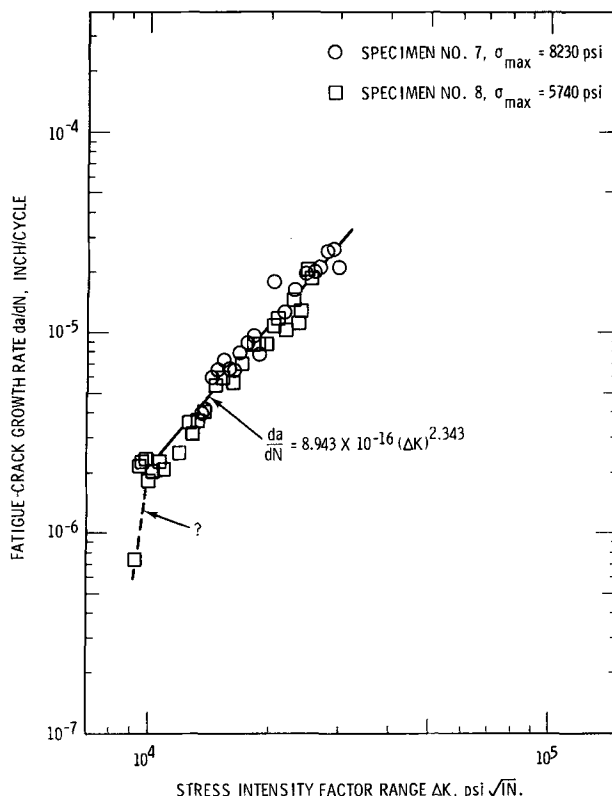


Fig. 5—Fatigue-crack propagation behavior of Type 304 stainless steel at 1000°F.

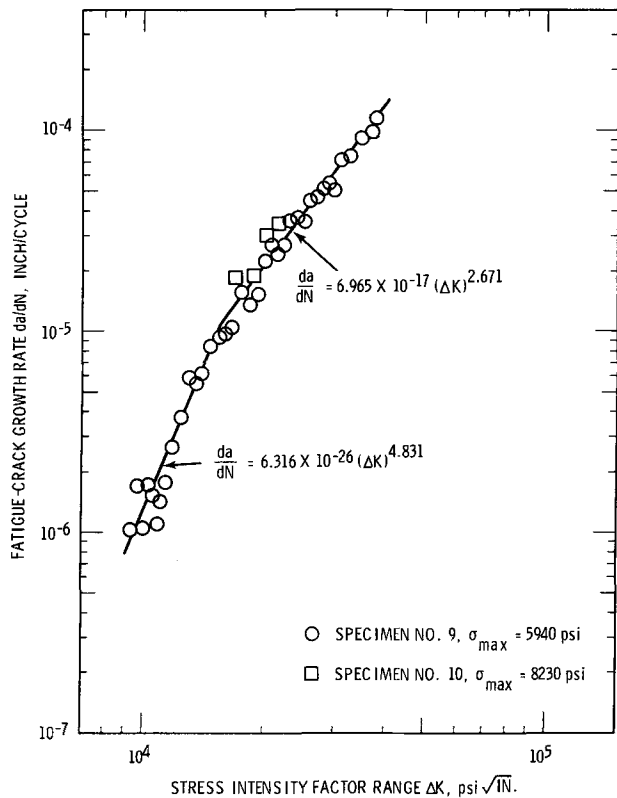


Fig. 6—Fatigue-crack propagation behavior of Type 304 stainless steel at 1200°F.

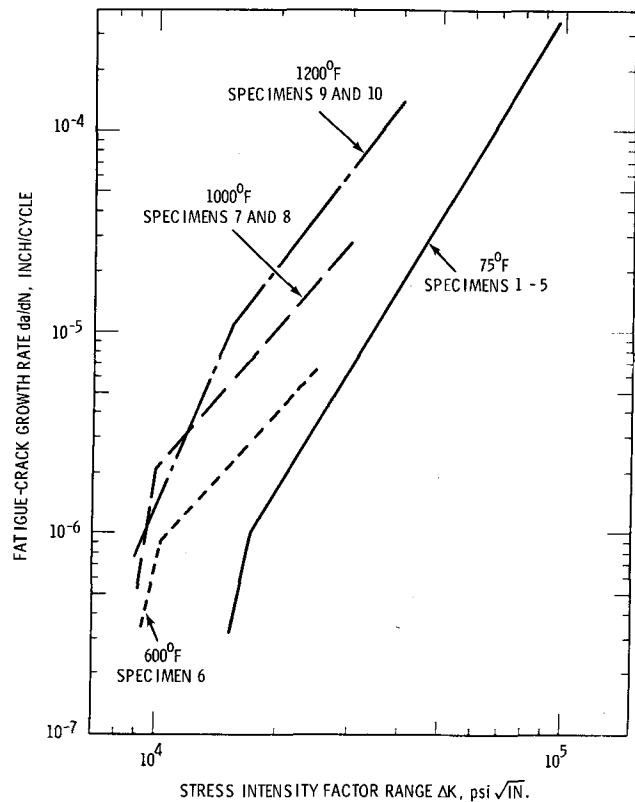


Fig. 8—Summary of fatigue-crack propagation behavior of Type 304 stainless steel.

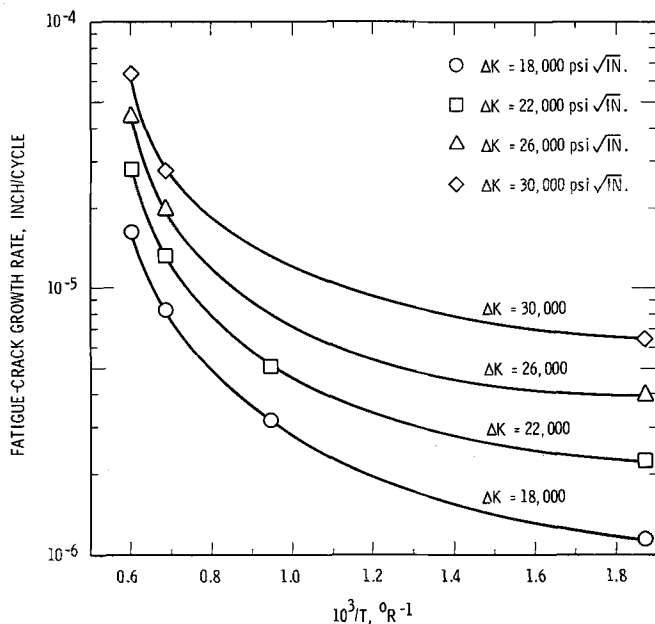


Fig. 7—Rate of fatigue-crack propagation as a function of the reciprocal of the test temperature.

upon the rate of fatigue-crack propagation. It appears that even at temperatures of approximately one-half the melting point,\* the simple power law relationship

\*1200°F corresponds to 1659°R, and the melting range of Type 304 stainless steel is 3009° to 3109°R.

of Eq. [3] holds so long as the average stresses in the

net section remain generally elastic. Actually, it appears necessary to use at least two power laws to adequately represent the behavior, as the data indicates that there is a transition in the  $da/dN$  vs  $\Delta K$  plot in the range  $\Delta K = 10,000$  to  $\Delta K = 17,000$  psi $\sqrt{\text{in.}}$ . The reason for this change in the cracking behavior is not known, but it is thought that the plastic zone size did not play a significant role since the transition takes place at essentially the same value of  $\Delta K$  at 75° and at 1200°F.

It has been previously suggested<sup>10, 11, 15</sup> that an Arrhenius-type rate process function might be used to describe the fatigue-crack growth behavior over a given temperature range. The results of the present study show, however, that a single rate process term does not describe the cracking behavior of Type 304 stainless steel over the temperature range 75° to 1200°F. The implication from this is that more than one process is dominant over this large temperature range, although final assessment of the application of rate process theory also hinges on a more complete definition of the preexponential term,  $A$ .

#### ACKNOWLEDGMENTS

This paper is based on work performed under U.S. Atomic Energy Commission Contracts AT(45-1)-2170 with WADCO Corp., and AT(45-1)-1830 with the Battelle-Memorial Institute.

The authors wish to express their appreciation to D. J. Criswell and R. T. Landsiedel, senior technicians at the WADCO Corp. and Battelle-Northwest respectively, who were most helpful in conducting the experiments in this study.

## APPENDIX

### Mechanical and Thermal History of Material

AISI Type 304 (Allegheny Ludlum Heat No. 55697) was poured into ingots which were 23 by 42 in. in cross-section. The ingots were subsequently hot rolled in thirty-three passes (starting temperature = 2350°F, finishing temperature = 2140°F) into slabs 6 in. thick by 36 in. wide.

After slabbing, the material was cut into three pieces for fabrication into the final product. The dimensions

of these pieces were 5.85 in. thick by 36 in. by 52 in. The pieces were reheated to 2250°F for 3½ hr prior to hot rolling. Hot rolling was accomplished in seventeen passes (starting temperature = 2250°F, finishing temperature = 1700°F) and the plates were reduced from a thickness of 5.85 in. to a thickness of 0.515 in.

After hot rolling, the plates were placed in a furnace at 1200°F and heated to 2000°F in 37 min. The material was held at 2000°F for 1 hr and then water quenched. The plates were then pickled, cut to size by abrasive cutting, and ultrasonically inspected.

## REFERENCES

1. W. F. Simmons and H. C. Cross: Am. Soc. Testing Mater., Spec. Tech. Publ. no. 124, 1952.
2. J. T. Berling and T. Slot: Am. Soc. Testing Mater., Spec. Tech. Publ. no. 459, 1969, pp. 3-30.
3. A. J. Brothers: Fatigue Crack Growth in Nuclear Reactor Piping Steels, Report GEAP-5607, General Electric Co., San Jose, 1968.
4. C. M. Hudson: Fatigue-Crack Propagation in Several Titanium and Stainless Steel Alloys and One Superalloy, NASA TN D-2331, 1961.
5. P. Paris and F. Erdogan: *J. Basic Eng.*, 1963, vol. 85, pp. 528-34.
6. P. C. Paris, R. A. Schmidt, and W. L. Weiss: Very Slow Fatigue Crack Crack Growth Rates in a Steel Alloy, presented at Third Natl. Symposium on Fracture Mech., Lehigh Univ., August 25-27, 1969; *Eng. Fract. Mech.*, in press.
7. D. P. Wilhem: Am. Soc. Testing Mater., Spec. Tech. Publ. no. 415, 1967, pp. 363-83.
8. T. R. Gurney: *Metal Cont. Brit. Weld. J.*, 1969, vol. 1, pp. 91-96.
9. J. A. Feeney, J. C. McMillan, and R. P. Wei: *Met. Trans.*, 1970, vol. 1, pp. 1741-57.
10. R. P. Wei: *Int. J. Fract. Mech.*, 1968, vol. 4, pp. 156-68.
11. J. T. Rider and J. P. Gallagher: *J. Basic Eng.*, 1970, vol. 92, pp. 121-25.
12. W. G. Clark, Jr. and H. E. Trout, Jr.: Influence of Temperature and Section Size on Fatigue Crack Growth Behavior in Ni-Mo-V Alloy Steel, presented at Second Natl. Symposium on Fracture Mech., Lehigh Univ., June 17-19, 1968; *Eng. Fract. Mech.*, in press.
13. L. A. James: *Nucl. Appl. Technol.*, 1970, vol. 9, pp. 260-67.
14. H. H. Smith, P. Shahinian, and M. R. Achter: *Trans. TMS-AIME*, 1969, vol. 245, pp. 947-53.
15. T. Yokobori: *Physics of Strength and Plasticity*, A. S. Argon, ed., pp. 327-38, M.I.T. Press, Cambridge, Mass., 1969.